「神経機能画像の進歩」2009年5月22日　仙台
9. 古川勝敏、藁谷正明、岡村信行、田代学、谷内一彦、古本祥三、工藤幸司、荒井啓行. 健常者、MCI、アルツハイマー病症例における FDG-PET と BF-227 アミロイド PET の検討. 第50回日本神経学会総会　2009年5月22日　仙台
10. 藁谷正明、岡村信行、古川勝敏、谷内一彦、工藤幸司、荒井啓行. アルツハイマー病早期診断における[11C]BF227-PET と VSRAD の比較研究. 第50回日本神経学会総会　2009年5月22日　仙台
11. 岡村信行. PET を用いたアルツハイマー病の超早期診断法の確立と普及について. 第15回 CYPRIS 技術交流会　2009年8月27日　東京
12. 岡村信行. 認知症の分子イメージング. 第49回日本核医学会学術総会　シンポジウム「脳疾患における分子イメージング」　2009年10月1日　旭川
13. 杉健太郎、岡村信行、石井賢二、石渡喜一、伊藤健吾、加藤隆司、鷲野谷利幸、工藤幸司、谷内一彦. [11C]BF227 を用いたアルツハイマー病早期診断法の多施設共同臨床試験. 第49回日本核医学会学術総会　2009年10月1日　旭川
14. 岡村信行、古本祥三、田代学、古川勝敏、杉健太郎、船木善仁、岩田錬、荒井啓行、工藤幸司、谷内一彦. アルツハイマー病診断における[18F]FACT-PET の有用性の検討. 第49回日本核医学会学術総会　2009年10月2日　旭川
15. 岡村信行. アミロイドイメージングの現状と展望. 第18回東北老年期認知症研究会　2009年11月14日　仙台
16. 岡村信行、古本祥三、荒井啓行、谷内一彦、工藤幸司. 神経原線維変化を検出する 18F 標識 PET プローブの開発. 第28回日本認知症学会学術集会　2009年11月20日　仙台
17. 藁谷正明、岡村信行、古川勝敏、谷内一彦、工藤幸司、荒井啓行. 軽度認知障害の予後予測における BF227-PET と MRI の比較検討. 第28回日本認知症学会学術集会　2009年11月20日　仙台
18. 岡村信行、古本祥三、田代学、古川勝敏、杉健太郎、荒井啓行、工藤幸司、谷内一彦. アミロイドイメージングプローブ[18F]FACT のアルツハイマー病早期診断における有用性の検討. 第16回東北脳循環カンファランス　2009年11月28日　仙台
19. 岡村信行、谷内一彦. 脳神経疾患におけるバイオマーカー. 第30回日本臨床薬理学会年会　ワークショップ1「臨床試験とバイオマーカー」　2009年12月3日　横浜

8. 知的財産権の出願・登録状況（予定も含む）

１. 特許取得

２. 実用新案登録
　なし
３. その他
　なし

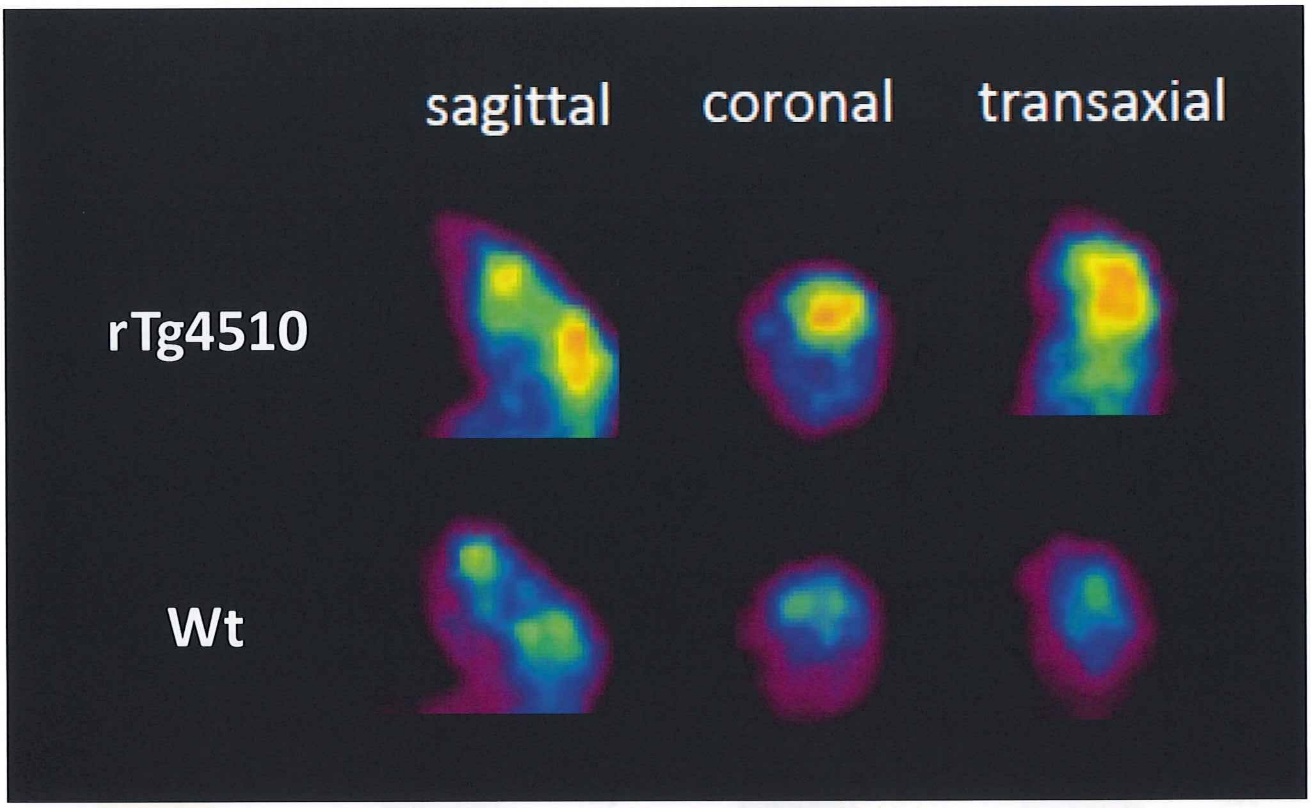

図1　タウトランスジェニックマウス（rTg4510）、野生型マウス（Wt）の[^{18}F]THK-5XX 投与 30 分後の PET 画像

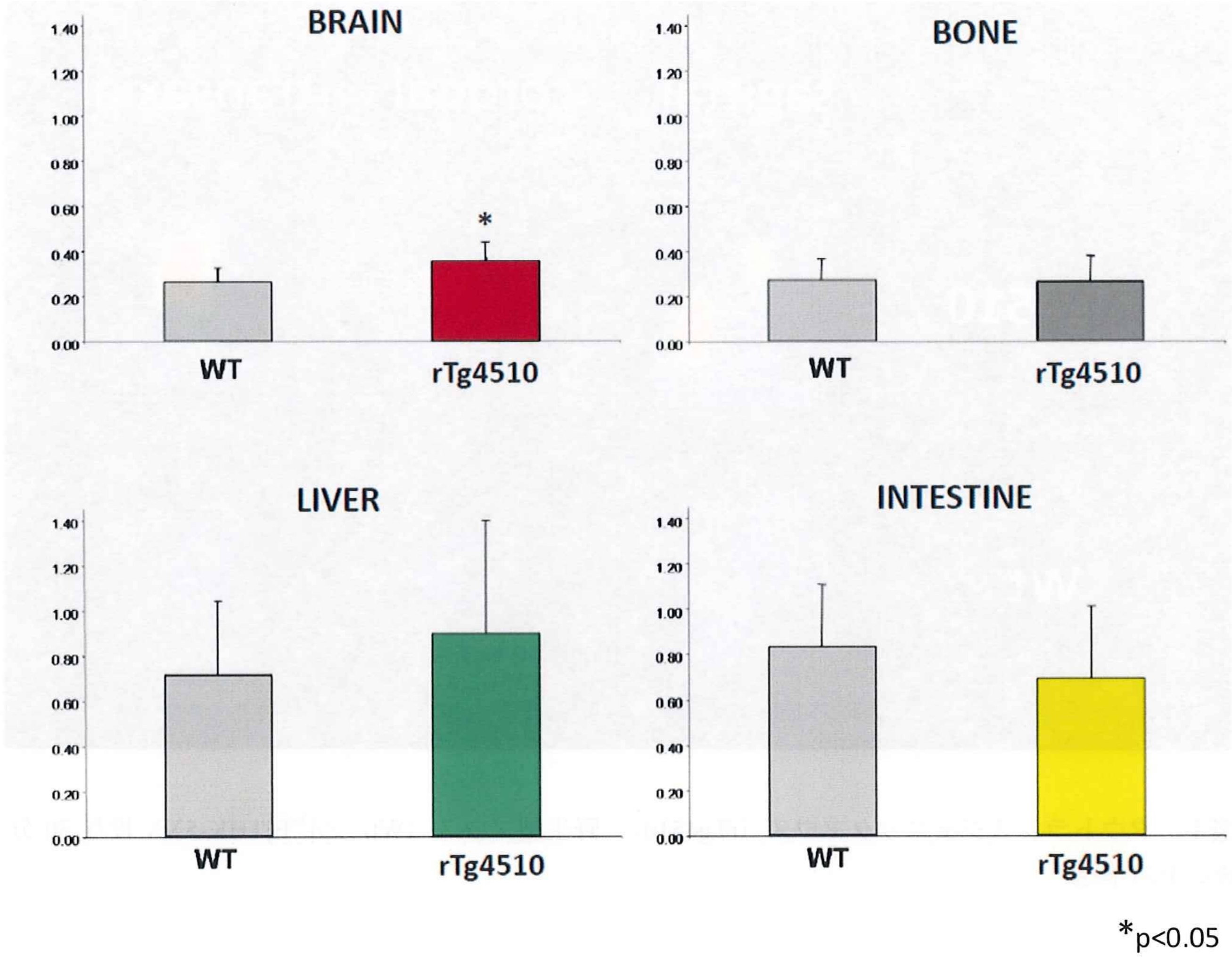

図２　タウトランスジェニックマウス（rTg4510）、野生型マウス（WT）における$[^{18}F]$THK-5XX 投与 30 分後の脳（Brain）、骨（Bone）、肝臓（Liver）、小腸（Intestine）のトレーサー集積量の比較

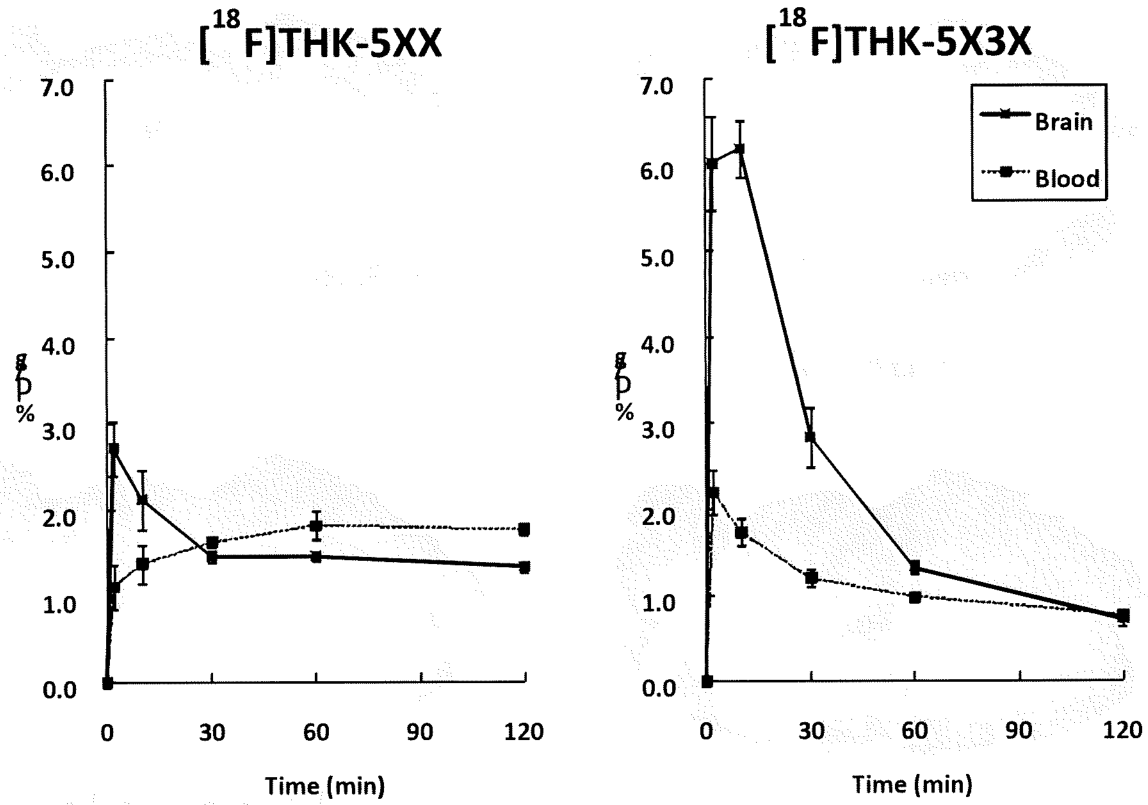

図３　正常（ICR）マウスにおける[18F]THK-5XX、[18F]THK-5X3X 静注後の脳および血液放射能量の時間変化

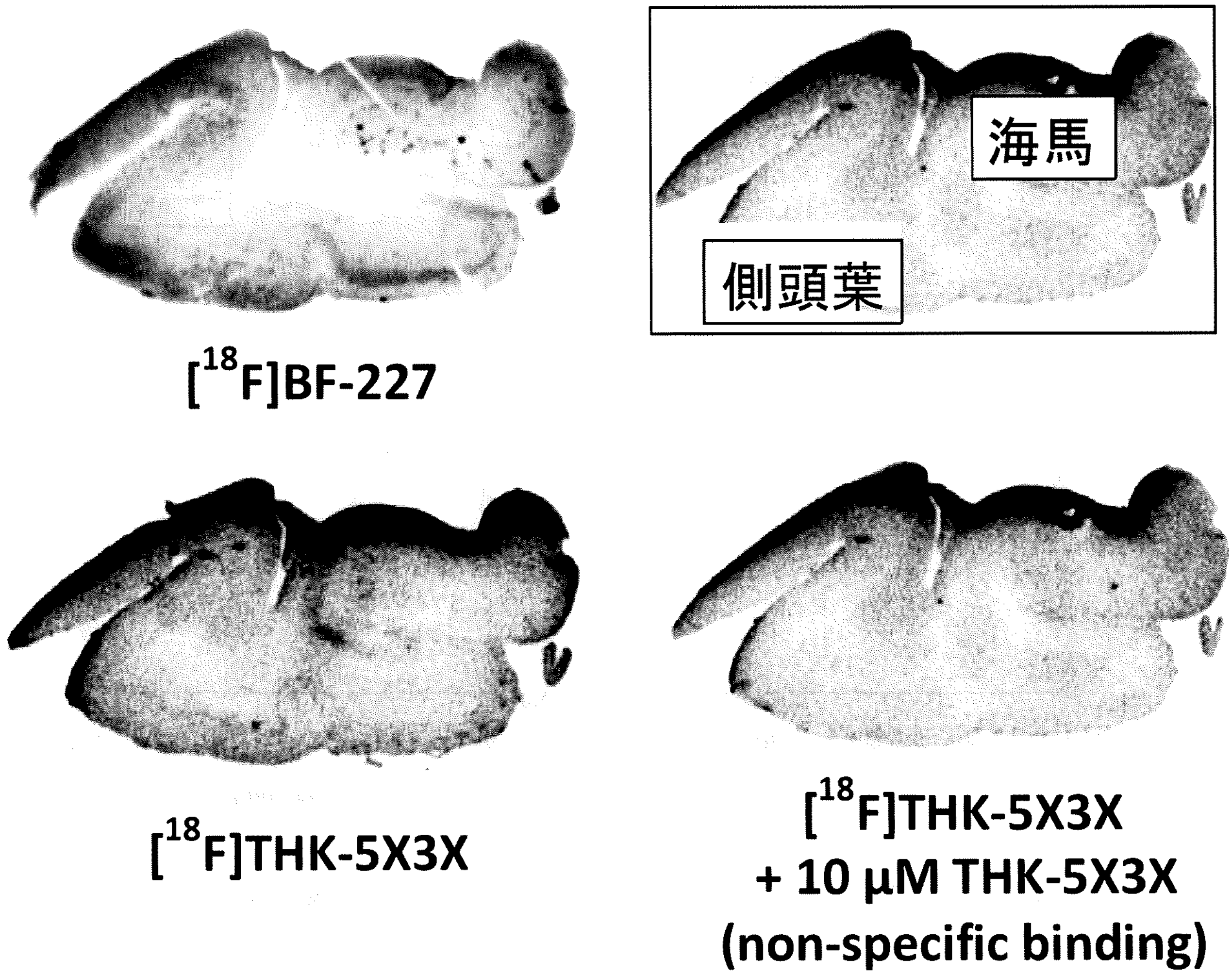

図４　$[^{18}F]$THK-5X3X、$[^{18}F]$BF-227 によるアルツハイマー病患者海馬ー側頭葉脳切片のオートラジオグラフィー像

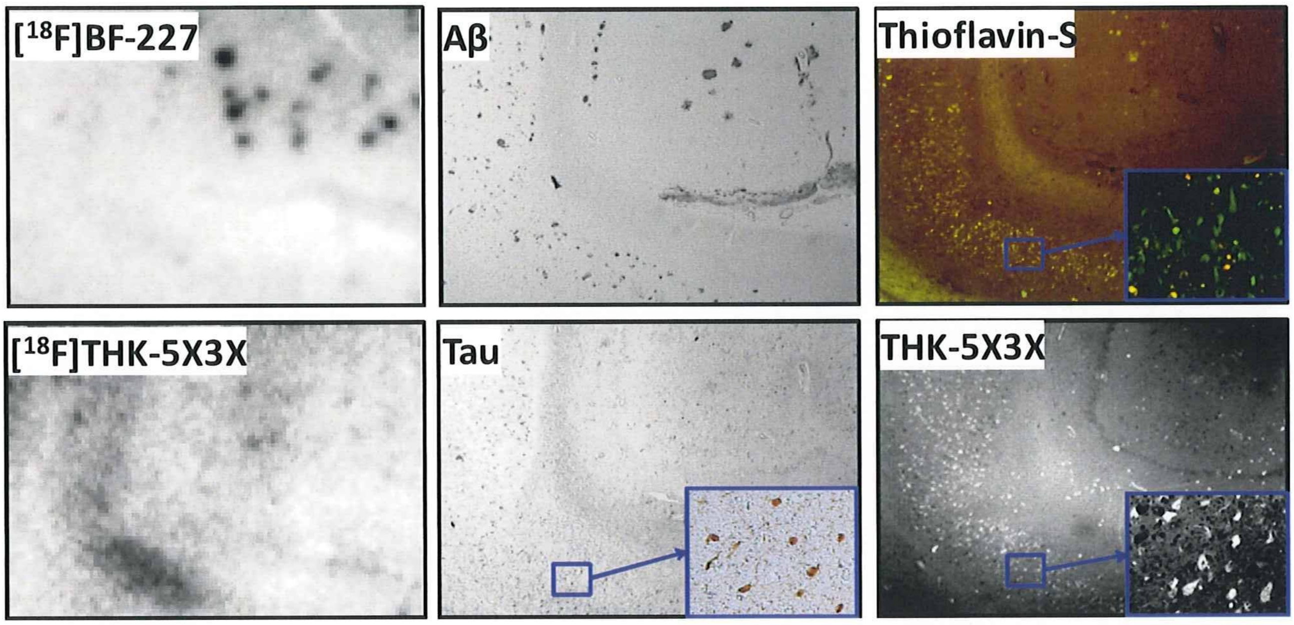

図５　[^{18}F]BF-227 、[^{18}F]THK-5X3X によるアルツハイマー病患者海馬脳切片のオートラジオグラフィーと免疫染色との比較

研究成果の刊行に関する一覧表

別紙４

研究成果の刊行に関する一覧表

書籍

著者氏名	論文タイトル名	書籍全体の編集者名	書　籍　名	出版社名	出版地	出版年	ページ
なし							

雑誌

発表者氏名	論文タイトル名	発表誌名	巻号	ページ	出版年
Okamura N, Shiga Y, Furumoto S, Tashiro M, Tsuboi Y, Furukawa K, Yanai K, Iwata R, Arai H, Kudo Y, Itoyama Y, Doh-ura K	In vivo detection of prion amyloid plaques using [11C]BF-227 PET	Eur J Nuc Med	37	934-941	2010
Kikuchi A, Takeda A, Okamura N, Tashiro M, Hasegawa T, Furumoto S, Kobayashi M, Sugeno N, Baba T, Miki Y, Mori F, Wakabayashi K, Funaki Y, Iwata R, Takahashi S, Fukuda H, Arai H, Kudo Y, Yanai K, Itoyama Y	In vivo visualization of {alpha}-synuclein deposition by carbon-11-labelled 2-[2-(2-dimethylaminothiazol-5-yl)ethenyl]-6-[2-(fluoro)ethoxy]benzoxazole positron emission tomography in multiple system atrophy.	Brain. Doi:10.1093/brain/awq091			2010
Furukawa K, Okamura N, Tashiro M, Waragai M, Furumoto S, Iwata R, Yanai K, Kudo Y, Arai H	Amyloid PET in mild cognitive impairment and Alzheimer's disease with BF-227: comparison to FDG-PET	J Neurol Doi10.1007/s00415-009-5396-8			2009
Waragai M, Okamura N, Furukawa K, Tashiro M, Furumoto S, Funaki Y, Kato M, Iwata R, Yanai K, Kudo Y, Arai H	Comparison study of amyloid PET and voxel-based morphometry analysis in mild cognitive impairment and Alzheimer's disease	J Neurol Sci.	285	100-105	2009
Fodero-Tavoletti MT, Mulligan RS, Okamura N, Furumoto S, Rowe CC, Kudo Y, Masters CL, Cappai R, Yanai K, Villemagne VL	In vitro characterisation of BF227 binding to alpha-synuclein/Lewy bodie	Eur J Pharmacol	617	54-58	2009

発表者氏名	論文タイトル名	発表誌名	巻号	ページ	出版年
Fujiwara H, Tabuchi M, Yamaguchi T, Iwasaki K, Furukawa K, Sekiguchi K, Ikarashi Y, Kudo Y, Higuchi M, Saido TC, Maeda S, Takashima A, Hara M, Yaegashi N, Kase Y, Arai H	A traditional medicinal herb Paeonia suffruticosa and its active constituent 1,2,3,4,6-penta-O-galloyl-beta-D-glucopyranose have potent anti-aggregation effects on Alzheimer's amyloid beta proteins in vitro and in vivo.	J Neurochem	1009	1648-1657	2009
Okamura N, Fodero-Tavoletti MT, Kudo Y, Rowe CC, Furumoto S, Arai H, Masters CL, Yanai K, Villemagne VL	Advances in molecular imaging for the diagnosis of dementia.	Expert Opin. Med. Diagn.	3	705-716	2009
荒井啓行、岡村信行、藁谷正明、古川勝敏、谷内一彦、工藤幸司	アルツハイマー病の病態とバイオマーカー開発	日薬理誌.	135	3-7	2010
工藤幸司	アミロイドーシスの分子イメージング	医学のあゆみ	299	430-435	2009

研究成果の刊行物・別刷

Eur J Nucl Med Mol Imaging (2010) 37:934–941
DOI 10.1007/s00259-009-1314-7

ORIGINAL ARTICLE

In vivo detection of prion amyloid plaques using [^{11}C]BF-227 PET

Nobuyuki Okamura · Yusei Shiga · Shozo Furumoto · Manabu Tashiro · Yoshio Tsuboi · Katsutoshi Furukawa · Kazuhiko Yanai · Ren Iwata · Hiroyuki Arai · Yukitsuka Kudo · Yasuhito Itoyama · Katsumi Doh-ura

Received: 7 August 2009 / Accepted: 21 October 2009 / Published online: 17 December 2009

Abstract

Purpose In vivo detection of pathological prion protein (PrP) in the brain is potentially useful for the diagnosis of transmissible spongiform encephalopathies (TSEs). However, there are no non-invasive ante-mortem means for detection of pathological PrP deposition in the brain. The purpose of this study is to evaluate the amyloid imaging tracer BF-227 with positron emission tomography (PET) for the non-invasive detection of PrP amyloid in the brain.

Methods The binding ability of BF-227 to PrP amyloid was investigated using autoradiography and fluorescence microscopy. Five patients with TSEs, including three patients with Gerstmann-Sträussler-Scheinker disease (GSS) and two patients with sporadic Creutzfeldt-Jakob disease (CJD), underwent [^{11}C]BF-227 PET scans. Results were compared with data from 10 normal controls and 17 patients with Alzheimer's disease (AD). The regional to pons standardized uptake value ratio was calculated as an index of BF-227 retention.

Results Binding of BF-227 to PrP plaques was confirmed using brain samples from autopsy-confirmed GSS cases. In clinical PET study, significantly higher retention of BF-227 was detected in the cerebellum, thalamus and lateral temporal cortex of GSS patients compared to that in the corresponding tissues of normal controls. GSS patients also showed higher retention of BF-227 in the cerebellum, thalamus and medial temporal cortex compared to AD patients. In contrast, the two CJD patients showed no obvious retention of BF-227 in the brain.

Conclusion Although [^{11}C]BF-227 is a non-specific imaging marker of cerebral amyloidosis, it is useful for in vivo detection of PrP plaques in the human brain in GSS, based on the regional distribution of the tracer. PET amyloid imaging might provide a means for both early diagnosis and non-invasive disease monitoring of certain forms of TSEs.

N. Okamura · S. Furumoto · K. Yanai
Department of Pharmacology,
Tohoku University School of Medicine,
Sendai, Japan

Y. Shiga · Y. Itoyama
Department of Neurology,
Tohoku University School of Medicine,
Sendai, Japan

S. Furumoto · R. Iwata
Division of Radiopharmaceutical Chemistry,
Cyclotron and Radioisotope Center, Tohoku University,
Sendai, Japan

M. Tashiro
Division of Cyclotron Nuclear Medicine,
Cyclotron and Radioisotope Center, Tohoku University,
Sendai, Japan

Y. Tsuboi
Department of Neurology,
Fukuoka University School of Medicine,
Fukuoka, Japan

K. Furukawa · H. Arai
Department of Geriatrics and Gerontology,
Division of Brain Sciences, Institute of Development,
Aging, and Cancer, Tohoku University,
Sendai, Japan

Y. Kudo
Innovation of New Biomedical Engineering Center,
Tohoku University,
Sendai, Japan

K. Doh-ura (✉)
Department of Prion Research,
Tohoku University School of Medicine,
2-1 Seiryo-machi, Aoba-ku, Sendai 980-8575, Japan
e-mail: doh-ura@mail.tains.tohoku.ac.jp

Keywords Prion · PET · Amyloid · Creutzfeldt-Jakob disease

Introduction

Transmissible spongiform encephalopathies (TSEs), also known as prion diseases, are a group of fatal neurodegenerative disorders, including Creutzfeldt-Jakob disease (CJD), Gerstmann-Sträussler-Scheinker disease (GSS) and kuru [1–3]. TSEs are characterized by progressive deposition of abnormal prion protein (PrP) in the brain. CJD is the most common type of human TSE and is classified into sporadic, genetic and infectious forms according to the aetiology of illness. GSS is a familial neurodegenerative disorder associated with mutations of the PrP gene and is clinically recognized by cerebellar ataxia combined with postural abnormalities and cognitive decline [1–3]. Two major types of abnormal PrP deposition, synaptic and plaque types, have been described in the brain of people with TSEs [1]. The synaptic type of PrP deposition, which does not have tinctorial properties of amyloid in tissue sections, is most commonly observed in sporadic CJD, whereas the plaque type, which frequently forms congophilic amyloid plaques, is a hallmark of such TSEs as GSS, variant CJD (vCJD) and iatrogenic dura CJD with plaques [1, 4]. Abnormal PrP deposition in the brain is suggested to start before the occurrence of clinical symptoms [5–7]. Thus, preclinical diagnosis and, when available, early disease-specific therapeutic interventions, can be beneficial for people predisposed to or affected by TSEs.

Several positron emission tomography (PET) imaging agents have been recently developed and used for in vivo detection of brain amyloid-β (Aβ) plaques in patients with Alzheimer's disease (AD) [8–12]. Most of these β-sheet binding agents show high binding affinity to PrP amyloid because PrP aggregates in TSEs form β-pleated sheet structures and share a common secondary structure with Aβ deposits in AD brains [13–16]. Therefore, these agents would be useful for the in vivo detection of PrP amyloid in the brain. Two clinical PET studies were performed using [^{18}F]FDDNP and/or [^{11}C]PIB in sporadic and familial CJD patients [17, 18]. The results indicated moderate retention of FDDNP and no obvious retention of PIB in the brain [17, 18]. Therefore, agents that can sensitively detect abnormal PrP deposits should be further explored for the diagnosis of TSEs. We have demonstrated in vitro and in vivo binding of benzoxazole derivatives to both Aβ and PrP amyloids [19, 20]. One of these derivatives, BF-227, was used for a clinical PET study where it successfully visualized amyloid deposits in the brain of AD patients in vivo [12, 21]. Therefore, [^{11}C]BF-227 appears to be a promising candidate for PET imaging of PrP deposits. The purpose of this study was to evaluate the clinical utility of [^{11}C]BF-227 PET for the non-invasive detection of abnormal PrP deposits in patients with TSEs.

Methods

Preparation of compounds

BF-227 and its 2-tosyloxyethoxy and *N*-desmethylated derivatives were custom synthesized by Tanabe R&D Service Co. (Osaka, Japan). [^{18}F]BF-227 was synthesized for autoradiography of brain sections, as described previously [22]. For the clinical studies, [^{11}C]BF-227 was synthesized as described previously [12]. Radiochemical yields were greater than 50% based on [^{11}C]methyl triflate, and specific radioactivities were 119–138 GBq/μmol at the end of synthesis. Radiochemical purities were greater than 95%.

Histopathological staining and in vitro autoradiography

Autopsy-diagnosed brain samples from two GSS cases with PrP plaque deposition and two sporadic CJD cases with synaptic PrP deposition were provided by Dr. Toru Iwaki of the Department of Neuropathology, Kyushu University, Japan. The brain sample from an 81-year-old man with autopsy-confirmed physiological aging was obtained from Tohoku University Hospital. The two GSS cases had a proline-to-leucine mutation at codon 102 and methionine homozygosity at codon 129 of the PrP gene, and the two sporadic CJD cases had no mutations and methionine homozygosity at codon 129; they showed type 1 abnormal PrP in immunoblotting of the brain tissues. All of the brain samples were treated with 98% formic acid for 1 h before paraffin embedding to eliminate prion infectivity. Sections from paraffin-embedded blocks of the cerebellum or frontal cortex were then dewaxed in xylene and ethanol. For staining with BF-227, tissue sections were immersed in 100 μM BF-227 solution containing 50% ethanol for 10 min. They were then dipped briefly into water and rinsed in phosphate-buffered saline for 10 min before coverslipping with FluorSave Reagent (Calbiochem, La Jolla, CA, USA). Subsequently, they were examined using an Eclipse E800 microscope (Nikon, Tokyo, Japan) equipped with a V-2A filter set (excitation, 380–420 nm; dichroic mirror, 430 nm; Longpass filter, 450 nm). For autoradiography, the section was incubated with 1.0 MBq/ml of [^{18}F]BF-227 at room temperature for 10 min and then washed briefly with water and 50% ethanol. After drying, the labelled section was exposed to a BAS-III imaging plate (Fuji Film, Tokyo, Japan) overnight. Autoradiographic images were obtained using a BAS-5000 phosphor imaging instrument (Fuji Film, Tokyo, Japan). Neighbouring sections were immunostained using 3F4 anti-PrP monoclonal antibody (Covance, Princeton, NJ, USA) as described previously [13, 20].

Subjects and patients in the clinical PET study

Five TSE patients, including two sporadic CJD patients [63-year-old woman (CJD1) and 58-year-old man (CJD2)] and three GSS patients [69-year-old woman (GSS1), 61-year-old man (GSS2) and 30-year-old woman (GSS3)], underwent PET scans with [^{11}C]BF-227 (Table 1). For comparison, [^{11}C]BF-227 PET studies were also performed in 17 AD patients [mean age ± standard deviation (SD)= 72.6±6.7; mean Mini-Mental State Examination score ± SD=19.8±4.0] and 10 aged normal controls (mean age ± SD=67.2±2.5). Some of these AD and normal subjects were included in our previous report [12].

CJD1's health was unremarkable until the manifestation of depressive symptoms at the age of 62 years. The patient then developed subacutely progressive dementia, motor disturbances and myoclonus. CJD2 showed subacutely progressive dementia and gait disturbance and then developed psychotic symptoms, dysarthria and myoclonus. Both CJD patients had no mutations and showed methionine homozygosity at codon 129 of the PrP gene. PET studies in CJD1 and CJD2 were performed when they reached grade 4 of the modified Rankin scale at 3 and 4 months after onset of symptoms, respectively. Both patients showed periodic synchronous discharges in electroencephalograms and hyperintensity in the caudate, putamen and cerebral cortex on diffusion-weighted magnetic resonance (MR) images. Diagnosis of probable CJD was made according to the WHO criteria [23].

Each GSS patient was from a different pedigree and had a family history of the same disease, carrying a proline-to-leucine mutation at codon 102 and methionine homozygosity at codon 129 of the PrP gene. GSS1 and GSS2, having a 9- and 20-month clinical duration from the onset, respectively, showed signs of moderate cerebellar ataxia, such as gait disturbance and slurred speech; however, they could walk unassisted and had slight or no cognitive impairment. GSS1 and GSS2 scored 22 and 26 points, respectively, on the Mini-Mental State Examination. GSS3, having a 27-month clinical duration, showed severe gait disturbance and slurred speech and was unable to walk unassisted; however, she had no cognitive impairment (30 points on the Mini-Mental State Examination) at the time of this study.

AD diagnosis was made according to the National Institute of Neurological and Communicative Diseases and Stroke-Alzheimer's Disease and Related Disorders Association (NINCDS-ADRDA) criteria [24]. CJD, GSS and AD patients were recruited from Miyagi National Hospital, Fukuoka University Hospital, Kagoshima University Hospital and Tohoku University Hospital. Normal controls were recruited from volunteers with no cognitive impairment or cerebrovascular lesions on MR images and who were not taking any centrally acting medications. No significant difference in age distribution was apparent between the groups. This study was approved by the Ethics Committee on clinical investigations of Tohoku University School of Medicine and performed in accordance with the Declaration of Helsinki. Written informed consent was obtained after complete description of the study to the patients and subjects.

Image acquisition protocols

PET scans were performed using a SET-2400W (Shimadzu Inc., Kyoto, Japan). After intravenous injection of 211–366 MBq (5.7–9.9 mCi) of [^{11}C]BF-227, dynamic PET images were obtained for 60 min with the subjects' eyes closed. Arterial blood sampling in the TSE patients was not

Table 1 Regional to pons standardized uptake value ratio (SUVRp) values in aged normal controls (Control), Alzheimer's disease patients (AD), Creutzfeldt-Jakob disease patients (CJD) and Gerstmann-Sträussler-Scheinker disease patients (GSS)

	Control (*n*=10) Mean ± SD	AD (*n*=17) Mean ± SD	CJD1	CJD2	GSS (*n*=3) Mean ± SD	GSS1	GSS2	GSS3
Frontal	0.60±0.03	0.64±0.04	0.57	0.61	0.67±0.08	0.74	0.69	0.57
Lateral temporal	0.59±0.03	0.69±0.04*	0.63	0.62	0.67±0.05*	0.71	0.68	0.61
Parietal	0.62±0.02	0.69±0.04*	0.62	0.62	0.67±0.06	0.72	0.68	0.61
Occipital	0.62±0.04	0.65±0.05	0.62	0.69	0.67±0.07	0.74	0.67	0.60
Medial temporal	0.64±0.04	0.62±0.03	0.57	0.65	0.67±0.02**	0.66	0.70	0.67
Striatum	0.71±0.04	0.75±0.04*	0.69	0.72	0.76±0.04	0.80	0.77	0.72
Thalamus	1.00±0.04	1.01±0.04	0.97	1.04	1.08±0.00*, **	1.08	1.07	1.08
Cerebellum	0.58±0.01	0.57±0.02	0.58	0.59	0.62±0.01*, **	0.61	0.63	0.61

*p<0.05 compared to aged normal group

**p < 0.05 compared to AD group

performed because the Committee on Clinical Investigation at Tohoku University School of Medicine did not approve blood sampling during the PET scan, from the standpoint of infection risk management. T_1-weighted MR images were obtained using a Signa 1.5-T machine (General Electric Inc., Milwaukee, WI, USA).

Image analysis

Standardized uptake value (SUV) images of [^{11}C]BF-227 were obtained by normalizing tissue concentration by injected dose and body weight. Average summations of SUV images were created from early frames (0–30 min post-injection) and late frames (40–60 min post-injection) of dynamic PET images. Early frame images were created for co-registration with individual MR images, and late frame images were used for calculation of SUV. Individual MR images were anatomically co-registered with the early frame PET images using statistical parametric mapping software (SPM2, Welcome Department of Imaging Neuroscience, London, UK) [25]. Spatial normalization was performed using an MR T_1 template of SPM2 to transfer PET images into a standard stereotactic space. Regions of interest (ROIs) were placed on a spatially normalized MR image, as described previously [12]. ROI information was then copied onto delayed PET SUV images, and regional SUV images at 40–60 min post-injection were sampled using Dr.View/LINUX software (AJS, Tokyo, Japan). Deposition of PrP plaques is reportedly frequent in the cerebellum but scarce in the pons of GSS brain [26]. Furthermore, BF-227 retention in the pons does not differ between AD patients and normal controls. Therefore, we used the pons as a reference region and calculated the regional to pons SUV ratio (SUVRp) as an index of BF-227 retention.

Statistical analysis

For statistical comparison in each group, we applied one-way analysis of variance, followed by the Bonferroni-Dunn post hoc test. Statistical comparison of age distribution was performed using the Kruskal-Wallis test, followed by Dunn's multiple comparison test. Statistical significance for each analysis was defined as $p<0.05$.

Results

Autoradiography examination indicated binding of a tracer dose of BF-227 to PrP plaque deposits. BF-227 retention was present in brain sections from GSS cases with PrP plaque deposition but not from normal control cases and sporadic CJD cases with synaptic PrP deposition (Fig. 1a–c). The regional distribution of [^{18}F]BF-227 in the autoradiograms co-localized with the immunostained PrP plaques in the cerebellar cortex of GSS cases (Fig. 1d–e). BF-227 binding to PrP plaques was additionally examined using a microscope, because BF-227 is a fluorescent compound. Core regions of the PrP plaques were intensely stained with BF-227 (Fig. 2, arrows), indicating that BF-227 preferentially binds to the fibril-rich core of PrP amyloid plaques.

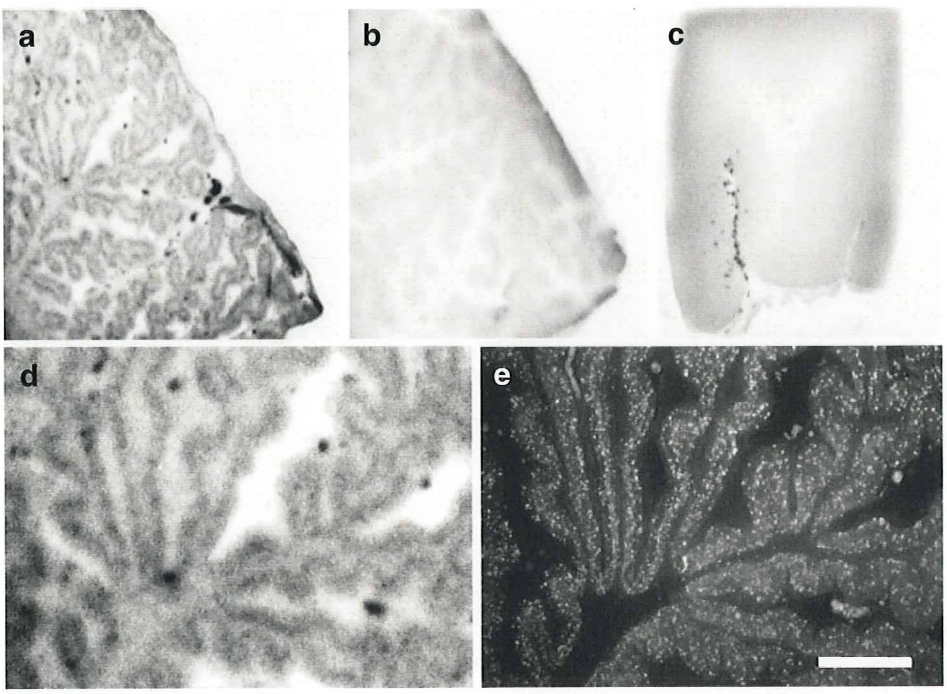

Fig. 1 [^{18}F]BF-227 autoradiograms of a cerebellar section from a Gerstmann-Sträussler-Scheinker (GSS) case (**a**), a cerebellar section from a physiological aging case (**b**) and a frontal cortex section from a sporadic Creutzfeldt-Jakob disease (CJD) case (**c**) are shown, together with a magnified view of **a** (**d**) and prion protein (PrP) immunostaining of the same field as **d** (**e**). BF-227 retention was present in the brain section from a GSS case with PrP plaque deposition, but not from a normal control case and sporadic CJD case with synaptic PrP deposition. *Bar*=200 μm

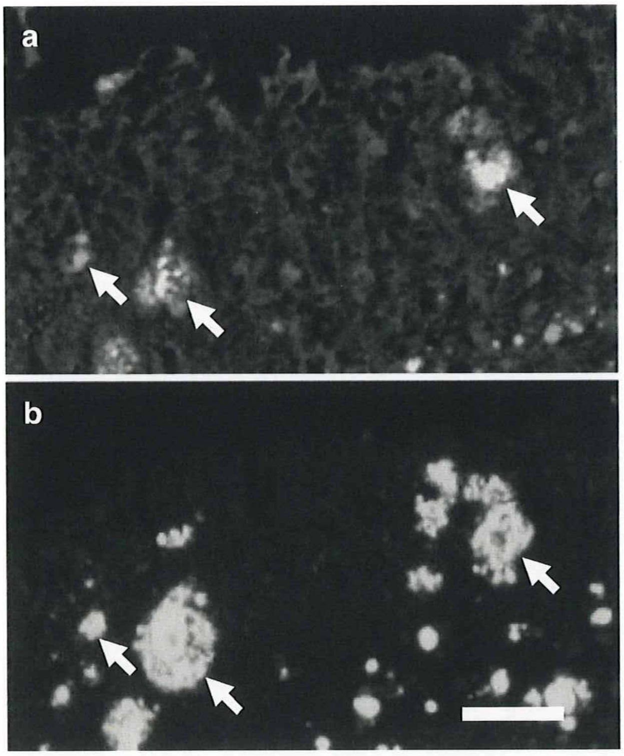

Fig. 2 Microscopic images of BF-227 staining (**a**) and PrP immunostaining (**b**) of the cerebellar cortex of a GSS case. *Arrows* indicate PrP amyloid plaques. The core regions of PrP plaques were intensely stained with BF-227. *Bar*=50 μm

Figure 3 shows the average summations of SUVRp images in an aged normal subject (64-year-old man), a sporadic CJD patient (CJD1, 63-year-old woman), a GSS patient (GSS2, 61-year-old man) and an AD patient (62-year-old woman). As reported previously, non-specific retention of [^{11}C]BF-227 was observed in the brain stem and white matter of all subjects [12]. The GSS patient showed obvious retention of [^{11}C]BF-227 in the cerebellum, and lateral and medial temporal cortices. The three GSS patients showed significantly higher SUVRp in the lateral temporal cortex, thalamus and cerebellum (Table 1, Fig. 4) when compared to aged normal controls. Furthermore, when compared to the AD group, the GSS group showed significant elevation of SUVRp in the medial temporal cortex, thalamus and cerebellum. Although two GSS patients (GSS1 and GSS2) showed retention of BF-227 in most brain regions, the youngest GSS patient (GSS3) showed BF-227 retention only in the cerebellum, thalamus and medial temporal cortex, but not in the neocortex (Table 1, Fig. 4). Furthermore, two sporadic CJD patients showed no obvious BF-227 retention in any of the brain regions examined (Table 1, Fig. 4). As previously described [12, 21], AD patients showed [^{11}C]BF-227 retention in the neocortex; however, the cerebellum and medial temporal cortex were relatively spared (Table 1).

Autopsy examination of the brain of one GSS patient (GSS1) confirmed both the presence of abundant PrP amyloid plaques in the neocortex, cerebellum, basal ganglia, thalamus, entorhinal cortex and hippocampus and the absence of Aβ amyloid plaques or other structures of misfolded protein deposition such as Lewy bodies and neurofibrillary tangles. When compared to controls, the highest SUVRp percentage difference was found in the neocortex, especially in the frontal cortex (22%), followed by the striatum (12%), thalamus (9%), cerebellum (6%) and medial temporal cortex (3%) in this case. This finding was consistent with the autopsy result showing higher density of PrP amyloid plaques in the neocortex and basal ganglia than in the cerebellum, thalamus and hippocampus. Details of clinicopathological features of this case will be published elsewhere.

Fig. 3 Mean regional to pons standardized uptake value ratio (SUVRp) images between 40 and 60 min post-injection of [^{11}C]BF-227 in an aged normal subject (64-year-old man), a sporadic CJD patient (CJD1, 63-year-old woman), a GSS patient (GSS2, 61-year-old man) and an AD patient (62-year-old woman). Compared to the aged normal subject and CJD patient, the GSS patient showed obvious [^{11}C]BF-227 retention in the cerebellum and temporal cortex. The AD patient also showed obvious [^{11}C]BF-227 retention in the temporal cortex; however, the cerebellum was relatively spared

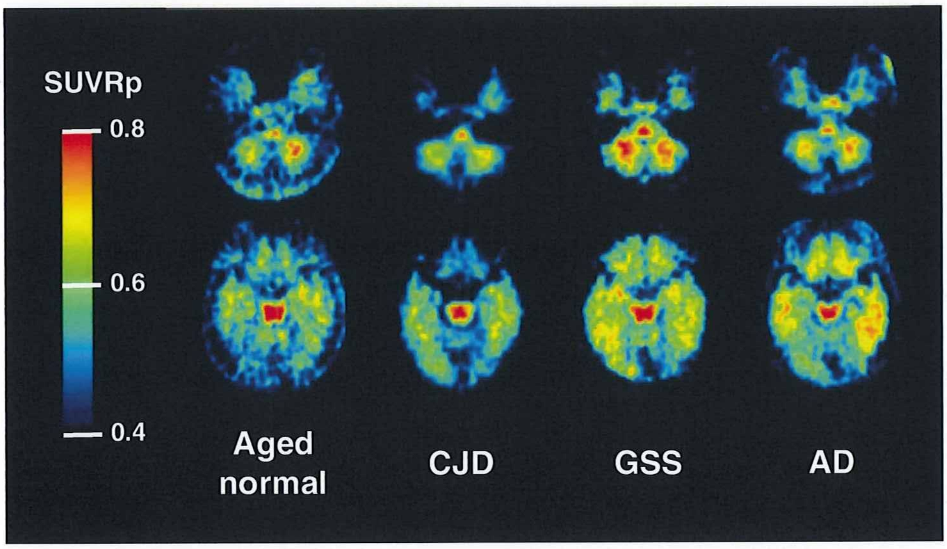

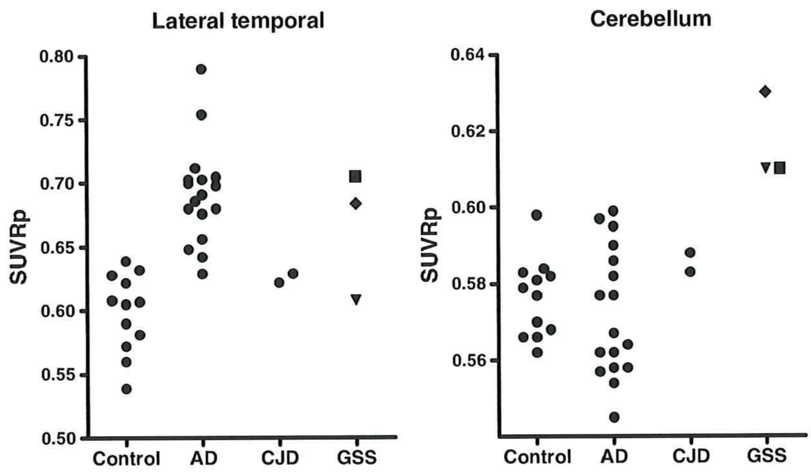

Fig. 4 SUVRp distribution in aged normal controls (*Control*), AD patients (*AD*), CJD patients (*CJD*) and GSS patients (*GSS*). GSS patients showed higher SUVRp values in the lateral temporal cortex and cerebellum. *Filled square* GSS1, *filled diamond* GSS2, *filled inverted triangle* GSS3

Discussion

This is the first study to demonstrate non-invasive detection of PrP amyloid plaques in GSS patients. GSS is neuropathologically characterized by deposits of multicentric amyloid plaques, which are especially abundant in the cerebellum, cerebral cortex and basal ganglia [3]. The present study demonstrated binding of BF-227 to PrP amyloid plaques in GSS brain sections. [^{11}C]BF-227 retention was observed in cortical and subcortical brain regions of GSS patients known for the high density of PrP plaques. Based on these findings, [^{11}C]BF-227 represents a promising candidate PET probe for the non-invasive detection of PrP amyloid plaques in the brain. However, the possibility that neocortical elevation of SUVRp in GSS patients might be caused by concomitant Aβ amyloid deposits or other misfolded protein deposits also should be considered, given that the two GSS patients showing prominent neocortical retention of [^{11}C]BF-227 were relatively older than the GSS patient showing no neocortical retention of BF-227. Although one positive GSS patient (GSS2) is still alive and was not examined neuropathologically, another positive case (GSS1) showed a high level of PrP amyloid deposits but no obvious deposits of Aβ amyloid or other misfolded proteins at autopsy. Furthermore, significant elevation of SUVRp was detected in the cerebellum, thalamus and hippocampus of all GSS cases. These brain regions are known to contain lower densities of Aβ plaques or other misfolded protein structures such as Lewy bodies. Based on these findings, it seems unlikely that concomitant deposition of Aβ amyloid or other misfolded proteins contributes to the high [^{11}C]BF-227 retention in GSS patients.

There is an increasing demand for in vivo detection of abnormal PrP deposition in the brain for the diagnosis of TSEs that might translate in early therapeutic intervention. Although GSS and other familial forms of TSEs can be diagnosed with PrP gene analysis using peripheral blood cells, it has been impossible to non-invasively measure the amount of abnormal PrP deposition in the brain. In a fashion similar to GSS, PrP amyloid deposition in the brain is commonly present in vCJD in which PrP amyloid plaques, called florid plaques, are pathognomonic [27]. Thus, [^{11}C]BF-227 PET might be a sensitive probe for the detection of PrP amyloid plaque deposition in vCJD as well as GSS, allowing longitudinal monitoring of PrP amyloid plaque deposition in the brain. Ante-mortem diagnosis of vCJD relies on the detection of abnormal PrP deposition in tonsil biopsy samples [28]. However, functional imaging using PET has an advantage over surgical biopsy tests in terms of both a non-invasive and an infection risk management point of view.

GSS is a rare form of TSE occurring in only about 3% of TSE cases in Japan. However, GSS is probably one of the TSEs most likely to benefit from early therapeutic interventions because the disease can be confirmed earlier using PrP gene analysis and progression occurs much more slowly than that in sporadic CJD, which comprises the majority of TSE cases. Recently, compounds such as pentosan polysulphate and doxycycline have been clinically used for experimental treatments for TSEs to prevent deposition of abnormal PrP in the brain, because these compounds slowed the disease progression in animal disease models when administered in an earlier stage of the disease [29–33]. Reliable surrogate markers are also required to evaluate the efficacy of these experimental interventions, and [^{11}C]BF-227 PET might be one of the best candidates to assess PrP amyloid deposition in GSS. However, it remains to be elucidated if PrP amyloid levels are a particularly relevant marker of therapeutic efficacy.

A previous PET study demonstrated moderate FDDNP retention and no remarkable PIB retention in the brain of two familial CJD patients with an octapeptide repeat insertion mutation [17]. A recent PET study has additionally demonstrated no PIB retention in two autopsy-confirmed sporadic

CJD patients [18]. In contrast with these studies, the present study successfully demonstrated prominent [^{11}C]BF-227 retention in the brain of GSS patients. Differences between the previous and present findings might mainly reside in the amount and type of PrP amyloid deposits in the brain, where histopathological studies indicate higher density of PrP amyloid plaques in GSS than in familial CJD [1]. In the present study, the findings in two sporadic CJD patients showing no obvious [^{11}C]BF-227 retention in the brain additionally support this speculation. The difference may also be attributable to higher binding affinity of BF-227 to PrP amyloid cores compared to FDDNP and PIB. To clarify this, further in vitro studies comparing the binding affinities of different amyloid tracers to PrP plaques in TSE brain homogenates are needed.

The youngest GSS patient (GSS3) showed BF-227 retention in the cerebellum and thalamus but not in the neocortex. The clinical symptoms in this patient were consistent with the brain distribution of BF-227, with the patient presenting with severe gait disturbance and slurred speech resulting from cerebellar ataxia but no signs of cognitive impairment, suggesting a close relationship between PrP plaque deposition as measured by BF-227 and regional brain dysfunction. There are variations of clinical phenotypes in GSS [1, 3]. Such variations are yet to be explained; however, the pattern of regional PrP amyloid distribution might be one of the factors affecting clinical phenotypes of GSS. In vivo PrP amyloid imaging using [^{11}C]BF-227 or other PET tracers will clarify neuropathological aspects of clinical variations in GSS.

In summary, we confirmed binding of BF-227 to PrP plaques in vitro and in vivo. A clinical PET study using [^{11}C]BF-227 demonstrated in vivo detection of PrP amyloid plaques in GSS patients. This imaging technique provides a potential means of facilitating both early diagnosis and non-invasive disease monitoring of certain forms of TSEs because, despite a lack of selectivity for PrP, brain retention of BF-227 in GSS shows a distinct pattern of regional distribution than that usually observed in sporadic AD.

Acknowledgment We appreciate the assistance of Dr. S. Watanuki, Dr. M. Miyake and Dr. H. Takashima in the clinical PET studies. This study was supported in part by the Program for the Promotion of Fundamental Studies in Health Science of the NIBIO in Japan, Industrial Technology Research Grant Program of the NEDO in Japan, and Health and Labor Sciences Research Grants (Translational Research and Research on Measures for Intractable Diseases) from the Ministry of Health, Labor, and Welfare of Japan.

References

1. DeArmond SJ, Kretzschmar HA, Prusiner SB. Prion diseases. In: Graham DI, Lantos PL, editors. Greenfield's neuropathology, 7th ed. London: Hodder Arnold. p. 273–323.
2. Collins SJ, Lawson VA, Masters CL. Transmissible spongiform encephalopathies. Lancet 2004;363:51–61.
3. Collins S, McLean CA, Masters CL. Gerstmann-Sträussler-Scheinker syndrome, fatal familial insomnia, and kuru: a review of these less common human transmissible spongiform encephalopathies. J Clin Neurosci 2001;8:387–97.
4. Noguchi-Shinohara M, Hamaguchi T, Kitamoto T, Sato T, Nakamura Y, Mizusawa H, et al. Clinical features and diagnosis of dura mater graft associated Creutzfeldt Jakob disease. Neurology 2007;69:360–7.
5. Lasmézas CI, Deslys JP, Demaimay R, Adjou KT, Hauw JJ, Dormont D. Strain specific and common pathogenic events in murine models of scrapie and bovine spongiform encephalopathy. J Gen Virol 1996;77(Pt 7):1601–9.
6. Schulz-Schaeffer WJ, Tschöke S, Kranefuss N, Dröse W, Hause-Reitner D, Giese A, et al. The paraffin-embedded tissue blot detects PrP(Sc) early in the incubation time in prion diseases. Am J Pathol 2000;156:51–6.
7. Fraser JR. What is the basis of transmissible spongiform encephalopathy induced neurodegeneration and can it be repaired? Neuropathol Appl Neurobiol 2002;28:1–11.
8. Small GW, Kepe V, Ercoli LM, Siddarth P, Bookheimer SY, Miller KJ, et al. PET of brain amyloid and tau in mild cognitive impairment. N Engl J Med 2006;355:2652–63.
9. Klunk WE, Engler H, Nordberg A, Wang Y, Blomqvist G, Holt DP, et al. Imaging brain amyloid in Alzheimer's disease with Pittsburgh Compound-B. Ann Neurol 2004;55:306–19.
10. Verhoeff NP, Wilson AA, Takeshita S, Trop L, Hussey D, Singh K, et al. In-vivo imaging of Alzheimer disease beta-amyloid with [11C]SB-13 PET. Am J Geriatr Psychiatry 2004;12:584–95.
11. Rowe CC, Ackerman U, Browne W, Mulligan R, Pike KL, O'Keefe G, et al. Imaging of amyloid beta in Alzheimer's disease with 18F-BAY94–9172, a novel PET tracer: proof of mechanism. Lancet Neurol 2008;7:129–35.
12. Kudo Y, Okamura N, Furumoto S, Tashiro M, Furukawa K, Maruyama M, et al. 2-(2-[2-Dimethylaminothiazol-5-yl]ethenyl)-6-(2-[fluoro]ethoxy)benzoxazole: a novel PET agent for in vivo detection of dense amyloid plaques in Alzheimer's disease patients. J Nucl Med 2007;48:553–61.
13. Ishikawa K, Doh-ura K, Kudo Y, Nishida N, Murakami-Kubo I, Ando Y, et al. Amyloid imaging probes are useful for detection of prion plaques and treatment of transmissible spongiform encephalopathies. J Gen Virol 2004;85:1785–90.
14. Bresjanac M, Smid LM, Vovko TD, Petric A, Barrio JR, Popovic M. Molecular-imaging probe 2-(1-[6-[(2-fluoroethyl)(methyl) amino]-2-naphthyl]ethylidene) malononitrile labels prion plaques in vitro. J Neurosci 2003;23:8029–33.
15. Sadowski M, Pankiewicz J, Scholtzova H, Tsai J, Li Y, Carp RI, et al. Targeting prion amyloid deposits in vivo. J Neuropathol Exp Neurol 2004;63:775–84.
16. Hoefert VB, Aiken JM, McKenzie D, Johnson CJ. Labeling of the scrapie-associated prion protein in vitro and in vivo. Neurosci Lett 2004;371:176–80.
17. Boxer AL, Rabinovici GD, Kepe V, Goldman J, Furst AJ, Huang SC, et al. Amyloid imaging in distinguishing atypical prion disease from Alzheimer disease. Neurology 2007;69:283–90.
18. Villemagne VL, McLean CA, Reardon K, Boyd A, Lewis V, Klug G, et al. 11C-PiB PET studies in typical sporadic Creutzfeldt-Jakob disease. J Neurol Neurosurg Psychiatry 2009;80:998–1001. doi:10.1136/jnnp.2008.171496.
19. Okamura N, Suemoto T, Shimadzu H, Suzuki M, Shiomitsu T, Akatsu H, et al. Styrylbenzoxazole derivatives for in vivo imaging of amyloid plaques in the brain. J Neurosci 2004;24:2535–41.
20. Ishikawa K, Kudo Y, Nishida N, Suemoto T, Sawada T, Iwaki T, et al. Styrylbenzoazole derivatives for imaging of prion plaques and treatment of transmissible spongiform encephalopathies. J Neurochem 2006;99:198–205.

21. Waragai M, Okamura N, Furukawa K, Tashiro M, Furumoto S, Funaki Y, et al. Comparison study of amyloid PET and voxel-based morphometry analysis in mild cognitive impairment and Alzheimer's disease. J Neurol Sci 2009;285:100–8. doi:10.1016/j.jns.2009.06.005.
22. Okamura N, Furumoto S, Funaki Y, Suemoto T, Kato M, Ishikawa Y, et al. Binding and safety profile of novel benzoxazole derivative for in vivo imaging of amyloid deposits in Alzheimer's disease. Geriatr Gerontol Int 2007;7:393–400.
23. Zeidler M, Gibbs CJ Jr, Meslin F. WHO manual for strengthening diagnosis and surveillance of Creutzfeldt-Jakob disease. Geneva: World Health Organization; 1998. p. 47–51.
24. McKhann G, Drachman D, Folstein M, Katzman R, Price D, Stadlan EM. Clinical diagnosis of Alzheimer's disease: report of the NINCDS-ADRDA Work Group under the auspices of Department of Health and Human Services Task Force on Alzheimer's Disease. Neurology 1984;34:939–44.
25. Friston KJ, Holmes AP, Worsley KJ, Poline JP, Frith CD, Frackowiack RSJ. Statistical parametric maps in functional imaging: a general linear approach. Hum Brain Mapp 1995;2:189–210.
26. Masters CL, Gajdusek DC, Gibbs CJ Jr. Creutzfeldt-Jakob disease virus isolations from the Gerstmann-Sträussler syndrome with an analysis of the various forms of amyloid plaque deposition in the virus-induced spongiform encephalopathies. Brain 1981;104:559–88.
27. Ironside JW, McCardle L, Horsburgh A, Lim Z, Head MW. Pathological diagnosis of variant Creutzfeldt-Jakob disease. APMIS 2002;110:79–87.
28. Hill AF, Zeidler M, Ironside J, Collinge J. Diagnosis of new variant Creutzfeldt-Jakob disease by tonsil biopsy. Lancet 1997;349:99–100.
29. Doh-ura K, Ishikawa K, Murakami-Kubo I, Sasaki K, Mohri S, Race R, et al. Treatment of transmissible spongiform encephalopathy by intraventricular drug infusion in animal models. J Virol 2004;78:4999–5006.
30. Rainov NG, Tsuboi Y, Krolak-Salmon P, Vighetto A, Doh-Ura K. Experimental treatments for human transmissible spongiform encephalopathies: is there a role for pentosan polysulfate? Expert Opin Biol Ther 2007;7:713–26.
31. De Luigi A, Colombo L, Diomede L, Capobianco R, Mangieri M, Miccolo C, et al. The efficacy of tetracyclines in peripheral and intracerebral prion infection. PLoS One 2008;3:e1888.
32. Teruya K, Kawagoe K, Kimura T, Chen CJ, Sakasegawa Y, Doh-ura K. Amyloidophilic compounds for prion diseases. Infect Disord Drug Targets 2009;9:15–22.
33. Forloni G, Salmona M, Marcon G, Tagliavini F. Tetracyclines and prion infectivity. Infect Disord Drug Targets 2009;9:23–30.

Brain Advance Access published April 29, 2010

doi:10.1093/brain/awq091

BRAIN
A JOURNAL OF NEUROLOGY

In vivo visualization of α-synuclein deposition by carbon-11-labelled 2-[2-(2-dimethylaminothiazol-5-yl)ethenyl]-6-[2-(fluoro)ethoxy]benzoxazole positron emission tomography in multiple system atrophy

Akio Kikuchi,[1] Atsushi Takeda,[1] Nobuyuki Okamura,[2] Manabu Tashiro,[3] Takafumi Hasegawa,[1] Shozo Furumoto,[2,4] Michiko Kobayashi,[1] Naoto Sugeno,[1] Toru Baba,[1] Yasuo Miki,[5] Fumiaki Mori,[5] Koichi Wakabayashi,[5] Yoshihito Funaki,[4] Ren Iwata,[4] Shoki Takahashi,[6] Hiroshi Fukuda,[7] Hiroyuki Arai,[8] Yukitsuka Kudo,[9] Kazuhiko Yanai[2] and Yasuto Itoyama[1]

1 Department of Neurology, Graduate School of Medicine, Tohoku University, Sendai, 980-8574 Japan
2 Department of Pharmacology, Graduate School of Medicine, Tohoku University, Sendai, 980-8575 Japan
3 Division of Cyclotron Nuclear Medicine, Cyclotron and Radioisotope Centre, Tohoku University, Sendai, 980-8578 Japan
4 Division of Radiopharmaceutical Chemistry, Cyclotron and Radioisotope Centre, Tohoku University, Sendai, 980-8578 Japan
5 Department of Neuropathology, Institute of Brain Science, Hirosaki University Graduate School of Medicine, Hirosaki, 036-8562 Japan
6 Department of Diagnostic Radiology, Graduate School of Medicine, Tohoku University, Sendai, 980-8575 Japan
7 Department of Nuclear Medicine and Radiology, Institute of Development, Ageing and Cancer, Tohoku University, Sendai, 980-8575 Japan
8 Department of Geriatric and Respiratory Medicine, Institute of Development, Ageing and Cancer, Tohoku University, Sendai, 980-8575 Japan
9 Innovation of New Biomedical Engineering Centre, Tohoku University, Sendai, 980-8574 Japan

Correspondence to: Atsushi Takeda,
Department of Neurology,
Graduate School of Medicine,
Tohoku University,
1-1 Seiryo-machi,
Aoba-ku, Sendai, Miyagi,
980-8574, Japan
E-mail: atakeda@em.neurol.med.tohoku.ac.jp

The histopathological hallmark of multiple system atrophy is the appearance of intracellular inclusion bodies, named glial cytoplasmic inclusions, which are mainly composed of α-synuclein fibrils. *In vivo* visualization of α-synuclein deposition should be used for the diagnosis and assessment of therapy and severity of pathological progression in multiple system atrophy. Because 2-[2-(2-dimethylaminothiazol-5-yl)ethenyl]-6-[2-(fluoro)ethoxy] benzoxazole could stain α-synuclein-containing glial cytoplasmic inclusions in post-mortem brains, we compared the carbon-11-labelled 2-[2-(2-dimethylaminothiazol-5-yl)ethenyl]-6-[2-(fluoro)ethoxy] benzoxazole positron emission tomography findings of eight multiple system atrophy cases to those of age-matched normal controls. The positron emission tomography data demonstrated high distribution volumes in the subcortical white matter (uncorrected $P < 0.001$), putamen and posterior cingulate cortex (uncorrected $P < 0.005$), globus pallidus, primary motor cortex and anterior cingulate cortex (uncorrected $P < 0.01$), and substantia nigra (uncorrected $P < 0.05$) in multiple system atrophy cases compared to the normal controls. They were coincident with glial cytoplasmic inclusion-rich brain areas in

Received January 13, 2010. Revised March 15, 2010. Accepted March 17, 2010.

multiple system atrophy and thus, carbon-11-labelled 2-[2-(2-dimethylaminothiazol-5-yl)ethenyl]-6-[2-(fluoro)ethoxy] benzoxazole positron emission tomography is a promising surrogate marker for monitoring intracellular α-synuclein deposition in living brains.

Keywords: glial cytoplasmic inclusion; Lewy body; β-amyloid; Parkinson's disease; Pittsburgh compound B

Abbreviations: BF-227 = 2-[2-(2-dimethylaminothiazol-5-yl)ethenyl]-6-[2-(fluoro)ethoxy]benzoxazole; MSA = multiple system atrophy; PIB = Pittsburgh compound B

Introduction

Multiple system atrophy (MSA) is a sporadic, progressive neurodegenerative disease characterized by variable severity of parkinsonism, cerebellar ataxia, autonomic failure and pyramidal signs. Although MSA was originally described as three separate diseases [olivopontocerebellar atrophy (Dejerine and Thomas, 1900), striatonigral degeneration (van der Eecken *et al.*, 1960) and Shy–Drager syndrome (Shy and Drager, 1960)], they are currently classified into a single disease that consists of MSA with predominant parkinsonism and MSA with predominant cerebellar ataxia (Gilman *et al.*, 1999). The histopathological hallmark of MSA, glial cytoplasmic inclusions, comprises mainly insoluble fibrils of phosphorylated α-synuclein (Wakabayashi *et al.*, 1998). Thus, it is suggested that the MSA is in the family of α-synucleinopathies (Marti *et al.*, 2003) including Parkinson's disease and dementia with Lewy bodies, which are characterized by the presence of Lewy bodies, representing other brain inclusions composed of α-synuclein.

Previous neuropathological studies indicated that the appearance of glial cytoplasmic inclusions preceded the clinical onset of MSA (Fujishiro *et al.*, 2008) and the amount of α-synuclein deposition correlated with the disease progression (Wakabayashi and Takahashi, 2006). Therefore, it is plausible that the formation of α-synuclein deposits plays a key role in neurodegeneration, and that compounds that inhibit this process may be therapeutically useful for MSA and other α-synucleinopathies. In fact some compounds, including antioxidants (Ono and Yamada, 2006) and non-steroidal anti-inflammatory drugs (Hirohata *et al.*, 2008), were reported to have potent anti-fibrillogenic and fibril-destabilizing effects on aggregated α-synucleins, and received much attention as possible new therapeutic agents (Ono and Yamada, 2006; Hirohata *et al.*, 2008). Detection of α-synuclein deposition *in vivo* could theoretically allow early diagnosis even at the presymptomatic stage, as well as assess disease progression and possible therapeutic effects in the living brain of patients with MSA.

Although Pittsburgh compound B (PIB) and other compounds were reported to be useful in detecting senile plaques *in vivo*, to our knowledge, there were no imaging probes currently available for *in vivo* detection of α-synuclein deposition. Recently, 2-[2-(2-dimethylaminothiazol-5-yl)ethenyl]-6-[2-(fluoro)ethoxy] benzoxazole (BF-227), known as a positron emission tomography (PET) probe for *in vivo* detection of dense β-amyloid deposits in humans (Kudo *et al.*, 2007), was reported to bind with synthetic α-synuclein aggregates as well as β-amyloid fibrils *in vitro* (Fodero-Tavoletti *et al.*, 2009). In the present study, we demonstrated that BF-227 could stain α-synuclein-containing glial cytoplasmic inclusions in post-mortem tissues and moreover, that a PET study with carbon-11-labelled BF-227 ([^{11}C]-BF-227) could detect α-synuclein deposits in the living brains of patients with MSA.

Materials and methods

Neuropathological staining

Brain specimens

The subjects of the first part of the study were nine autopsy cases, including three with Parkinson's disease, three with dementia with Lewy bodies and three with MSA. The above diagnoses were confirmed both clinically and histopathologically. Brain tissues taken from the temporal cortex and substantia nigra of patients with Parkinson's disease and dementia with Lewy bodies, and pontine base of patients with MSA, were fixed in 20% buffered formalin for 72 h at 4°C, and vibratome sections (50 μm thick) were prepared.

Fluorescence and immunohistochemical analysis

BF-227 was dissolved in 50% ethanol containing 5% polysorbate (Tween 80; Wako, Osaka, Japan). The sections were slide mounted, incubated in 100 μM BF-227 for 30 min, dipped three times in phosphate buffer, and coverslipped with non-fluorescent mounting medium (Vectashield, Vector Laboratories, Burlingame, CA, USA). Fluorescence images were visualized using an Olympus Provis fluorescence microscope (Olympus, Tokyo, Japan) at wavelength 400 nm. After photographing fluorescent structures, BF-227-labelled sections were immunostained with primary antibodies against phosphorylated α-synuclein (#64; Wako). For phosphorylated α-synuclein immunohistochemistry, the sections were pre-treated with 99% formic acid for 5 min, then incubated overnight at 4°C with each primary antibody followed by incubation with the biotinylated secondary antibodies and the avidin–biotin–peroxidase complex (Vectastain ABC kit, Vector Laboratories). Diaminobenzidine was used as the chromogen.

PET study

Subjects

Eight patients with probable MSA and eight age-matched normal subjects were studied to examine the distribution of [^{11}C]-BF-227 in the brain. All probable MSA patients were diagnosed on the second consensus criteria for probable MSA (Gilman *et al.*, 2008). Table 1 summarizes the clinical features of these patients. There were no significant differences in age, disease duration and unified MSA rating scale score between the MSA with predominant parkinsonism